1 **Article type: Original Article**

2 **Full Title: ZmCLA4 regulates leaf angle through multiple plant**

3 **hormone-mediated signal pathways in maize**

4 **Running title: ZmCLA4 regulates leaf angle**

5 Dandan Dou[a], Shengbo Han[a], Lixia Ku[a*], Huafeng Liu, Huihui Su, Zhenzhen Ren, Dongling

6 Zhang, Haixia Zeng, Yahui Dong, Zhixie Liu, Fangfang Zhu, Qiannan Zhao, Jiarong Xie, Yajing

7 Liu, Haiyang Cheng, Yanhui Chen*

8 College of Agronomy, Synergetic Innovation Center of Henan Grain Crops and National Key

9 Laboratory of Wheat and Maize Crop Science, Henan Agricultural University, No. 15 Longzihu

10 University Park, Zhengdong New Area, Zhengzhou, Henan, 450046, China

11 [a]These authors contributed equally to this work

12 *Correspondence should be addressed to Y.C. (chy9890@163.com), or L. K.

13 (kulixia0371@163.com)

14

15

16

17

18

19

20

Abstract

Leaf angle in cereals is an important agronomic trait contributing to plant architecture and grain yield by determining the plant compactness. Although ZmCLA4 was identified to shape plant architecture by affecting leaf angle, the detailed regulatory mechanism of ZmCLA4 in maize remains unclear. ZmCLA4 was identified as a transcriptional repressor using the Gal4-LexA/UAS system and transactivation analysis in yeast. The DNA affinity purification (DAP)-seq assay showed that ZmCLA4 not only acts as a repressor containing the EAR motif (CACCGGAC), but was also found to have two new motifs, CCGARGS and CDTCNTC. On analyzing the ZmCLA4-bound targeted genes, we found that ZmCLA4, as a cross node of multiple plant hormone-mediated pathways, directly bound to ARF22 and IAA26 to regulate auxin transport and mediated brassinosteroid signaling by directly binding to BZR3 and 14-3-3. ZmCLA4 bound two WRKY genes involved with abscisic acid, two genes (CYP75B1, CYP93D1) involved with jasmonic acid, B3 involved in the response to ethylene, and thereby negatively regulated leaf angle formation. We built a new regulatory network for the *ZmCLA4* gene controlling leaf angle in maize, which contributed to the understanding of ZmCLA4's regulatory mechanism and will improve grain yields by facilitating optimization of plant architecture.

Key words: DNA affinity purification (DAP)-Seq, leaf angle, maize, regulatory mechanism, regulatory network

Introduction

In the past few decades, improvement in plant architecture, especially the varieties with erect leaves, has played an important role in the genetic gain of maize yield (Lambert *et al.*, 1978; Tian *et al.*, 2011). Upright leaves may have the additional benefit of reducing shade from neighboring plants, thereby increased planting density (Dubois and Brutnell, 2011). Therefore, it is an important selection target for ideal plant type breeding to have an upward leaf angle, and of great significance to clarify the genetic basis of the leaf angle for ideal maize breeding.

Research over the past several decades has identified quantitative trait loci (QTL) that regulate leaf angle by using bi-parental populations (Mickelson *et al.*, 2002; Lu *et al.*, 2007; Ku *et al.*, 2010, 2012; Chen *et al.*, 2015; Li *et al.*, 2015), and nested association mapping populations (Tian *et al.*, 2011) in maize. Taking advantage of 3D images from potted plants grown under greenhouse conditions, QTL analyses have been performed in maize using leaf angle data collected throughout the canopy at different developmental stages (McCormick *et al.*, 2016; Zhang *et al.*, 2017). QTLs explained between 0.45% and 85% of the phenotypic variance. Tian *et al.* (2019) mapped 12 QTLs for leaf angle in a population of 866 maize–teosinte BC_2S_3 recombinant inbred lines derived from a cross between the maize inbred line W22 and the teosinte accession CIMMYT 8759. To date, in the multiple QTLs that have been located, only six genes have been reported as a result of the combined use of quantitative genetics (Ku *et al.*, 2011; Zhang *et al.*, 2014; Ren *et al.*, 2020; Tian *et al.*, 2019; Cao *et al.*, 2020). The first reported candidate gene, *ZmTAC1*, on a major QTL

for LA that was detected on chromosome 2, was cloned using a comparative genomics method (Ku *et al*., 2011). A nucleotide mutation in the 5′-untranslated region (UTR) influenced *ZmTAC1* expression (Ku *et al*., 2011). UPA1 (Upright Plant Architecture1) and UPA2, two QTLs conferring upright plant architecture, were cloned by map-based cloning (Tian *et al*., 2019). UPA2 is controlled by a two-base sequence polymorphism that regulates the expression of a B3-domain transcription factor (ZmRAVL1) located 9.5 kilobases downstream. UPA2 exhibits differential binding by DRL1 (DROOPING LEAF1), and DRL1 physically interacts with *LG1* (LIGULELESS1) and represses LG1 activation of ZmRAVL1. ZmRAVL1 regulates brd1 (brassinosteroid C-6 oxidase1), which underlies UPA1, altering endogenous brassinosteroid content and leaf angle (Tian *et al*., 2019). *ZmILI1*, a candidate gene of qLA2 on chromosome 2, directly binds to the promoters of the downstream gene *LG1* and activates *LG1* to further increase leaf angle (Ren *et al*., 2020). Ren *et al*. (2020) also found that *ZmILI1* and CYP90D1 formed a negative feedback loop to maintain the balance of brassinolide in maize. Cao *et al*. (2020) demonstrated that ZmIBH1-1 cloned by a map-based method negatively regulated leaf angle by causing cell wall lignification and cell elongation in the ligular region in maize.

In our previous study, ZmCLA4 cloned by a map-based method (Zhang *et al*., 2014) was identified as the ortholog of LAZY1 in rice and *Arabidopsis*. ZmCLA4 plays a negative role in the control of the maize leaf angle through the alteration of mRNA accumulation, leading to altered shoot gravitropism and cell development. In rice, LAZY1 regulates rice shoot gravitropism and tiller/leaf angle through an

asymmetrical auxin pathway, which affects auxin transport, leading to its asymmetrical distribution (Li *et al*., 2007; Yoshihara and Iino, 2007). Zhang *et al.* (2018) demonstrated through transcriptome analysis that HSFA2D acts as a positive regulatory protein and plays a role upstream of LAZY1, and two transcription factors, WOX6 and WOX11, which are functionally redundant, play a role downstream of the LAZY1 signaling pathway in rice. Chen *et al.* (2011) showed that OsPIN2-overexpressing plants suppressed the expression of the gravitropism-related gene *OsLAZY1* in shoots, but did not alter the expression of OsPIN1b and OsTAC1, which were reported as tiller angle controllers. Li *et al*. (2019) showed that OsBRXL4 regulated shoot gravitropism by affecting polar auxin transport, similar to LAZY1. From the sequence analysis of AtLAZY1, Yoshihara *et al*. (2013) demonstrated that the functional domains inferred were nuclear localization signals, located between regions III and IV, and an EAR motif located in conserved region V. EAR motifs are often found in transcription regulators, and in many cases function as repressors (Kazan, 2006; Kagale *et al*., 2010). Although the identification and characterization of ZmCLA4 have increased our understanding of the role of gravitropism in shaping plant architecture, the detailed molecular mechanism involved in the regulation of polar auxin transport by LAZY1 remains unclear in plants. In this study, ZmCLA4 was identified as a transcriptional repressor using the Gal4-LexA/UAS system and transactivation analysis in yeast. The DNA affinity purification (DAP)-Seq assay showed that ZmCLA4, acting as a repressor, contained the EAR motif (CACCGGAC) and two new motifs (CCGARGS and CDTCNTC). Through the analysis of targeted

genes bound by ZmCLA4, acting as a cross node of multiple plant hormone-mediated signaling pathways, ZmCLA4 not only directly bound to ARF22 and IAA26 to regulate auxin transport but also mediated brassinosteroid signal transduction by directly binding to BZR3 and 14-3-3. Additionally, it bound WRKYs involved with abscisic acid (ABA), two genes (CYP75B1, CYP93D1) involved with jasmonic acid (JA), and B3 involved in the response to ethylene, and thereby affected leaf angle formation. The results contributed to a better understanding of the ZmCLA4 regulatory pathways.

Materials and methods

Plant materials

The ZmCLA4-RNAi-transgenic (ZmCLA4-RT) line, with Yu368 as the genetic background, and the wild-type (WT) line (Zhang *et al.*, 2014) were sown in 2018. During the growth of the ZmCLA4-RT and WT lines, a sample from the leaf pulvinus in the 9-, 10-, and 11-leaf stages were obtained for each, immediately frozen in liquid nitrogen, and stored at -80°C before RNA/DNA extraction for molecular characterization and determination of the molecular mechanism of ZmCLA4.

Transcriptional activation assay in yeast

The yeast strain YRG-2 (Stratagene, USA) containing the HIS3 and lacZ reporter genes was used to test transcriptional activation activity. The coding sequences (CDS) of ZmCLA4 were inserted into the pBD-GAL4 vector via EcoRI/SmaI sites, in which ZmCLA4 was fused with the GAL4 binding domain. The pBD-ZmCLA4, pBD-GAL4 (negative controls), and pGAL4 (positive control) plasmids were

131 independently transfected into YRG-2 cells. The transfected yeast cells were grown
132 on YPDA medium or SD/-Trp/-His medium for 3 d at 30 °C. β-Galactosidase filter
133 assays were also conducted to determine the β-galactosidase activity of the transfected
134 yeast cells by monitoring the generation of blue color, according to the method
135 described in the Yeast Protocols Handbook (PT3024-1).

136 **Gal4/UAS System assay**

137 35S-ZmCLA4 contains the cauliflower-mosaic virus (CaMV) 35S promoter, which
138 drives ZmCLA4 expression. 35S-Luciferase contains firefly luciferase driven by the
139 constitutive CaMV-35S promoter. The reporter gene constructs (UAS-GUS) and
140 effector constructs (VP16, Gal4, and IAA17) were described previously by Tiwari *et*
141 *al*. (2001). The ZmCLA4-GAL4 effector construct contains the full-length ZmCLA4
142 coding sequence fused to the N-terminus of the Gal4 DNA-binding domain under the
143 control of the CaMV-35S promoter. The 35S-LUC construct was co-transformed as
144 an internal control to normalize the GUS reporter gene expression. GUS and LUC
145 enzymatic assays were performed in *Nicotiana benthamiana* leaves and performed
146 according to Gampala *et al*. (2001).

147 **DAP-Seq experiments**

148 DAP-Seq experiments were performed following the method described by O'Malley
149 *et al.* (2016). First, a DAP-seq genomic DNA (gDNA) library was prepared by
150 attaching a short DNA sequencing adaptor onto purified and fragmented gDNA. The
151 adapter sequences were truncated Illumina TruSeq adapters; the TruSeq Universal
152 and Index adapters corresponded to the DAP-seq Adapter A,

CACGACGCTCTTCCGATCT, and Adapter B, GATCGGAAGAGCACACGTCTG. The DAP gDNA library was prepared using the kit from NEBNext® DNA Library Prep Master Mix Set for Illumina® (NEB #E6040S/L). ZmIBH1-1 was fused to HaloTag using the kit from pFN19K HaloTag T7 SP6 Flexi Vecto (cat#G184A) (Promega). ZmCLA4 fused to HaloTag was expressed using the TnT SP6 High-Yield Wheat Germ Protein Expression System (L3260) (Promega), and then purified using Magne HaloTag Beads (G7281) (Promega) and Magne HaloTag Beads. Next, the ZmCLA4-HaloTag mixture was incubated with 500 ng DNA library in 40 ul PBS buffer with slow rotation in a cold room for 1.5 h. The beads were washed five times with 200 μL PBS + NP40 (0.005%), and then were resuspended into the PBS buffer. The supernatant was removed and 25 μL of the EB buffer was added and incubated for 10 min at 98 °C to elute the bound DNA from the beads. The correct DAP-Seq library concentration to achieve a specific read count was calculated based on the library fragment size. Negative control mock DAP-Seq libraries were prepared as described above but without the addition of protein to the beads.

DAP-Seq data analysis

We defined target genes as those that contained DAP-Seq peaks located within the transcribed regions of genes, in introns, 3 kb upstream of the transcription start site (TSS), or 3 kb downstream of the transcription termination site. DAP-Seq reads were aligned to the maize genome using Bowtie 2 (Langmead and Salzberg, 2012). Bowtie 2 supports the gapped and paired-end alignment modes. We ran Bowtie version 2.2.3 with default parameters and reported unique alignments. DAP-Seq peaks were

detected using MACS2 (Zhang *et al.*, 2008). We used MACS version 2.0.10, with default parameters because duplicates were allowed, with the q-value < 0.05.

Electrophoretic mobility shift assay

The full-length ZmCLA4 cDNA was amplified with gene primers (Supplementary Table S1) and fused into the *Sgf*I and *Pme*I sites of pFN19K HaloTag® T7 SP6 Flexi® Vector. The HaloTag-CLA4 fusion protein was expressed using the TNT® Coupled Wheat Germ Extract Systems (Promega, Fitchburg, WI, USA) and Magne® HaloTag Beads (Promega) EMSA. Oligonucleotide probes (Supplementary Table S1) were synthesized and labeled according to the standard protocol of Invitrogen Technology (Shanghai, China). We used standard reaction mixtures for the EMSA containing 20 ng of purified ZmCLA4 fusion protein, 5 ng of biotin-labeled annealed oligonucleotides, 2 μL of 10× binding buffer (100 mM Tris, 500 mM KCl, and 10 mM DTT, pH 7.5), 1 μL of 50% (v/v) glycerol, 1 μL of 100 mM $MgCl_2$, 1 μL of 1 mg mL^{-1} poly(dI– dC), 1 μL of 1% (v/v) Nonidet P-40, and double-distilled water to obtain a final volume of 20 μL. The reactions were incubated at 25 °C for 20 min, electrophoresed in 6% (w/v) polyacrylamide gels, and then transferred to N+ nylon membranes (Millipore, Darmstadt, Germany) in 0.53× TBE (Tris-Borate–EDTA) buffer at 380 mA and 4 °C for 30 min. Biotin-labeled DNA was detected using the LightShift™ Chemiluminescent EMSA kit (Thermo Fisher). Bands were visualized using the Chemiluminescent Western Blot Detection Kit (Thermo Fisher).

Transient assays for *in vivo* activation activity

To generate the Pro CLA4, luciferase (LUC) reporters for the dual-luciferase assays, ~2500 bp from the TSS promoter region of potential targets for stress response, were inserted into pGreenII0800-LUC. To generate the CaMV 35S promoter-driven ZmCLA4 effector, the full-length coding sequence of ZmCLA4 was inserted into pUC18-35S. Transient dual-luciferase assays were performed in *N. benthamiana* leaves and checked using dual-luciferase assay reagents (Promega). Following infiltration, plants were maintained at room temperature under a 14/10 h light/dark photoperiod. Leaf protein was extracted 48 h later. The protein was extracted using a passive lysis buffer (Cat# E1910, Promega). LUC activity was measured using a GloMax®20/20 Luminometer (Cat# E5311, Promega). Then, 100 µL of Stop and Glow Buffer was added to the reaction and Renilla luciferase (REN) activity was measured. For this analysis, the ratio between LUC and REN activities was measured three times.

Real-time reverse transcription-PCR (qRT-PCR)

Total RNA was isolated from the collected samples using TRIzol reagent (Invitrogen, Waltham, MA, USA) and treated with RNase-free DNase I to remove DNA contamination. cDNA was synthesized using an M-MLV reverse transcriptase-based cDNA first-strand synthesis kit (Invitrogen). qRT-PCR was performed using the SYBR® Green CR Master Mix Kit (Applied Biosystems, Waltham, MA, USA), following the manufacturer's protocol on a LightCycler® 480II Sequence Detection System. Relative gene expression was calculated according to the $2^{-\Delta\Delta Ct}$ method.

Expression values were normalized to the *18S* ribosomal gene for qRT-PCR. The primer sequences used in the qRT-PCR assay are listed in Supplementary Table S1.

Results

ZmCLA4 acts as a transcription repressor

A previous study identified ZmCLA4 with some sequence similarity to the rice gene OsLAZY1 and Arabidopsis gene AtLAZY1 (Li *et al*., 2007; Dong *et al*., 2013; Yoshihara *et al*., 2013; Zhang *et al*., 2014). The only functional domain inferred from the sequence analysis of ZmCLA4 was an ethylene-responsive element binding factor-associated amphiphilic repression (EAR) motif located in the conserved region (Figure 1A) and was frequently identified at the C-terminal end of the protein (Ohta *et al*., 2001). EAR motifs are often found in transcription regulators, and in many cases, function as repressors (Kazan, 2006; Kagale *et al*., 2010). To confirm that ZmCLA4 can activate or inhibit gene expression as a transcription factor, ZmCLA4 was first subjected to transactivation analysis in yeast. The results showed that ZmCLA4 had no transcriptional activation activity in yeast (Figure 1B). We then used the Gal4-LexA/UAS system, which tests ZmCLA4 for positive or negative transcriptional potential (Tiwari *et al*., 2001). The reporter gene was expressed at high levels when co-transformed into protoplasts with the LexAVP16 fusion construct, which contained the coding sequences for the LexA DNA-binding domain fused in frame with the coding sequence of the VP16 transcriptional activation domain. As reported previously (Tiwari *et al*., 2001), Gal4 fusion with the transcriptional repressor domain

of IAA17 (IAA17a1) strongly reduced the expression of the reporter gene. Similarly, the co-transformation of the reporter gene with a construct for the ZmCLA4-Gal4 fusion protein (ZmCLA4-Gal4) significantly decreased reporter gene expression (Figure 1C). Together, these results demonstrate that ZmCLA4 is a transcriptional repressor.

DAP-Seq identifies genes directly targeted by ZmCLA4

To investigate the regulatory mechanism mediated by *ZmCLA4*, we performed a DAP-Seq assay to uncover the genes directly targeted by ZmCLA4. Using the Illumina platform (50 bp-long pair-end reads), the DAP-Seq assay produced ~2.8 million reads for each sample, of which ~2.1 million reads were uniquely mapped to the maize_V4 genome sequence with an effective read ratio of ~75% (Table S2). We predicted ZmCLA4 binding sites using the software MACS2 (Zhang *et al*., 2008) with a p-value < 0.05 (based on a Poisson distribution comparing the ZmCLA4 sample and the control) and identified 7182 peaks across the entire genome through the ZmCLA4 binding motifs CACCGGAC, CCGARGS, and CDTCNTC (Figure 2A). Of the ZmCLA4 binding sites, 49.44% (3524 peaks) were located in the genic regions containing the genes, as well as 3 kb upstream of the start codon and 3 kb downstream of the stop codon (Figure 2B, C). Among these genic region peaks, 35.62%, 1.25%, 12.34%, 14.63%, and 36.16% are located in the promoter, 5′ -UTRs, introns, exons, and the transcription termination region, respectively.

The 3524 peaks corresponded to 3128 genes. Stringent Gene Ontology (GO) term enrichment analysis of the 3128 genes revealed that ZmCLA4 binding genes are

mainly involved in the regulation of biological processes, multicellular organismal processes, development, signaling, responses to stimuli, and regulation of cell proliferation, among others (Figure 2D). More specifically, ZmCLA4 binds to the upstream region of 1114 genes involved in biological regulation, signaling, regulation of cell proliferation, and response to stimuli. Of the 1114 genes bound to the upstream regions, 16 genes appeared to be responsible for the leaf angle. These genes were involved in response to phytohormones, such as ABA, auxin, and brassinolide (Table S3).

Binding Motif Analysis Revealed Novel ZmCLA4 cis-Elements

To confirm that ZmCLA4 was bound to the predicted EAR cis-element (CACCGGAC), an EMSA was performed using a purified ZmCLA4 protein and a labeled DNA probe containing the ZmCLA4-binding site (CACCGGAC). As shown in Figure 2E, ZmCLA4 bound to CACCGGAC. The addition of an 80× unlabeled competitor reduced the detected binding of ZmCLA4, and it did not bind to mutant probes (CACCGGAC mutated into TCTTTTGT). Without the ZmCLA4 protein, no bands were observed, except for the free probe. These results further confirmed the specific binding of ZmCLA4 to CACCGGAC.

To explore novel ZmCLA4 binding motifs, the 3 kb flanking sequences around all of the genic peak summits were applied to the motif discovery tool MEME-ChIP. The motifs CCGARGS and CDTCNTC were identified as statistically defined motifs (E-Value = 9.1 e-222, E-Value = 1.1 e-308, respectively; Figure 2A). Cis-element scanning was performed using the CCGARGS and CDTCNTC motifs on the 3 kb

283 flanking sequences around the peak maxima, and 1086 potential ZmCLA4 directly
284 targeted genes with functional annotations were detected. Among the 1086 genes, 195
285 were in the promoter regions and combined with CCGARGS and CDTCNTC.
286 Confirming the labeled DNA probe contained the ZmCLA4-binding sites,
287 CCGARGS and CDTCNTC, Figure 2E shows ZmCLA4 bound to CCGAAGC and
288 CTTCGTC. Furthermore, the addition of the 80× unlabeled competitor reduced the
289 detected binding of ZmCLA4, and it did not bind to mutant probes (CCGAAGC and
290 CTTCGTC mutated into TTCTTAT and AACGTTAGT, respectively). Without the
291 ZmCLA4 protein, no bands were observed, except for the free probe. These results
292 confirmed the specific binding of ZmCLA4 to CCGAAGC and CTTCGTC.

293 **ZmCLA4 regulates auxin transport by directly binding to ARF and IAA**
294 **transcription factors in maize**

295 Li *et al.* (2007) and Yoshihara *et al.* (2007) demonstrated that OsLAZY affects rice
296 shoot gravitropism and tiller/leaf angle by negatively regulating auxin transport,
297 leading to the asymmetric distribution of auxin. ZmCLA4, an ortholog of OsLAZY,
298 was identified to directly bind to auxin response factors (Zm00001d036593, ARF22;
299 Zm00001d039513, IAA26; Table S3). To understand whether ZmCLA4 functions as
300 a transcriptional repressor of the auxin-respective genes, we performed a
301 dual-luciferase transient transcriptional activity assay using *N. benthamiana* leaves
302 with ZmCLA4 driven by the cauliflower-mosaic virus (CaMV) 35S promoter as an
303 effector and LUC (the firefly luciferase-coding gene driven by -500- to -3000
304 auxin-respective genes) as the reporter gene (Figure 3A). The results showed that

ZmCLA4 specifically repressed the expression of LUC with the ARF22 promoter and increased the expression of LUC with the IAA26 promoter, indicating that the two genes are target genes of ZmCLA4 **(**Figure 3B). Additionally, we found that ZmCLA4 binds to three ABC transporter G family members (Zm00001d042953, ABC-2; Zm00001d009243, MRP10; Zm00001d023392, ABCG37; Table S3) mediating the efflux of the auxin precursor. The results showed that ZmCLA4 specifically repressed the expression of LUC with the ABC-2 promoter, MRP10 promoter, and ABCG37 promoter, indicating that these genes are the target genes of ZmCLA4 **(**Figure 3B).

To understand the effects of ZmCLA4 on ARF22, IAA26, ABC-2, MRP10, and ABCG37 *in vivo*, we measured mRNA levels of the five genes by qRT-PCR in WT and ZmCLA4-RNAi plants. The ZmCLA4 was expressed in the WT but not in ZmCLA4-RNAi plants in leaf pulvinus of 9-leaf, 10-leaf, and 11-leaf, whereas mRNA levels of ARF22, ABC-2, MRP10, and ABCG37 were significantly higher, and the mRNA level of IAA26 was significantly lower in the leaf pulvini of the ZmCLA4-RNAi plants than in WT plants **(**Figure 3B). These results were consistent with the expression results of LUC with corresponding gene promoters.

ZmCLA4 mediates brassinosteroid signal transduction by directly binding to BZR3 and 14-3-3 in maize

Among the genes bound by ZmCLA4, there are two genes (Zm00001d053543 and BZR3; Zm00001d003401, 14-3-3; Table S3) involved in brassinosteroid signal transduction. We performed dual-luciferase transient transcriptional activity assays

with the ZmCLA4 protein and LUC driven by the promoter sequences of the two genes as reporters (Figure 3A). The results showed that ZmCLA4 specifically repressed the expression of LUC with the BZR3 promoter and increased the expression of the 14-3-3 promoter, indicating that the two genes are target genes of ZmCLA4 **(**Figure 4A).

To further understand the effects of ZmCLA4 on BZR3 and 14-3-3 *in vivo*, we measured mRNA levels of the two genes by qRT-PCR in WT and ZmCLA4-RNAi plants. The mRNA level of BZR3 was significantly higher in leaf pulvini of the ZmCLA4-RNAi plants than in the WT in the 9-leaf, 10-leaf, and 11-leaf. The mRNA level of 14-3-3 was significantly lower in leaf pulvini of the ZmCLA4-RNAi plants than in WT plants in the 9-leaf, 10-leaf, and 11-leaf **(**Figure 4A). These results were consistent with the expression results of LUC with corresponding gene promoters.

ZmCLA4 directly regulates other phytohormone-respective genes

In this study, we also found that ZmCLA4 binds to four genes (Zm00001d035167, GTE8; Zm00001d050723, SnRK2.6; Zm00001d013240, WRKY4; Zm00001d003331, WRKY72) in response to ABA, two genes (Zm00001d047425, CYP75B1; Zm00001d046758, CYP93D1) associated with JAs, two genes (Zm00001d024545, B3; Zm00001d007522, ETO1) involved in the response to ethylene. We performed dual-luciferase transient transcriptional activity assays to investigate whether ZmCLA4 could function as a repressor of these genes. The results showed that LUC expression driven by GTE8, SnRK2.6, WRKY4, WRKY72, CYP75B1, CYP93D, B3,

and ETO1 promoters was prominently induced by ZmCLA4 **(**Figure 5A), indicating that these genes are the target genes of ZmCLA4.

To further understand the effects of ZmCLA4 on GTE8, SnRK2.6, WRKY4, WRKY72, CYP75B1, CYP93D, B3, and ETO1 *in vivo*, we measured the mRNA levels of the eight genes by qRT-PCR in WT and ZmCLA4-RNAi plants. The mRNA levels of SnRK2.6, WRKY4, WRKY72, CYP75B1, CYP93D, B3, and ETO1 were significantly higher in leaf pulvini of the ZmCLA4-RNAi plants than in the WT in the 9-leaf, 10-leaf, and 11-leaf, and the mRNA level of GTE8 was significantly lower in leaf pulvini of the ZmCLA4-RNAi plants than in the WT in the 9-leaf, 10-leaf, and 11-leaf **(**Figure 5B). These results were consistent with the expression results of LUC with corresponding gene promoters.

Discussion

Leaf angle is a key agronomic trait determining maize plant architecture and grain yield per unit area. Maize plant architecture with more upright leaves (i.e., smaller leaf angle) decreases mutual shading and sustains light capture for photosynthesis; thus, increasing the accumulation of leaf nitrogen for grain filling and increasing grain yield. ZmCLA4 plays a negative role in the control of maize LA through the alteration of mRNA accumulation. However, the regulatory mechanism of ZmCLA4 has not been reported in maize. In this study, sequence analysis showed that ZmCLA4 acts as a repressor including an EAR motif located in the conserved region. First, we identified that ZmCLA4 had no transcriptional activation activity through transactivation analysis in yeast. Then, ZmCLA4 was identified as a transcriptional

repressor through the Gal4-LexA/UAS system. The EAR motif was located at the C-terminal end of the AtLAZY1 protein (Yoshihara *et al*., 2013), whereas the conclusion was not proved by corresponding experiments in *Arabidopsis*. The results of the DAP-Seq assay showed that ZmCLA4 directly affected the expression of target genes through binding motifs CACCGGAC (EAR motif), CCGARGS, and CDTCNTC. This result not only further proved that ZmCLA4 acts as a repressor containing the EAR motif, but also identified two new motifs (CCGARGS and CDTCNTC), thereby providing a solid basis for further analysis of the molecular characteristics of ZmCLA4.

In rice, OsLAZY1 plays a negative role in polar auxin transport (PAT), and loss-of-function of OsLAZY1 greatly enhances PAT; thus, altering the endogenous IAA distribution in shoots, leading to reduced gravitropism, and the leaf/tiller-spreading phenotype of rice plants (Li *et al*., 2007). However, the detailed molecular mechanism involved in the regulation of PAT by LAZY1 is still unclear. In this study, ZmCLA4, an ortholog of OsLAZY, directly bound to auxin response factors ARF22 and IAA26 to participate in the auxin signal transduction pathway TIRI/AFB-Aux/IAA/TPL-ARFs, thereby affecting PAT. The auxin receptor TIR1 and its homologous receptor protein AFBs interact with Aux/IAA protein, which is an inhibitor of auxin signaling. Then, auxin stabilizes TIRI/AFB and Aux/IAA protein interaction, and degrades Aux/IAA protein, thus releasing ARFs, which are inhibited by the Aux/IAA protein, to mediate auxin signal transduction (Dharmasiri *et al*., 2005 *a*, *b*; Kepinski and Leyser, 2005 *a*, *b*). ARFs are important for the normal growth and

development of plants. In *Arabidopsis*, they control leaf development. ARF5 is critical to leaf initiation and vein pattern formation (Garrett *et al*., 2012). OsARF19-overexpression lines show an enlarged lamina inclination (leaf angle increase) because of an increase in its adaxial cell division in rice (Zhang *et al*., 2015). Our qRT-PCR results showed that the mRNA level of ARF22 was significantly higher and that of IAA26 was significantly lower in the leaf pulvini of the ZmCLA4-RNAi plants than in WT plants. Additionally, ZmCLA4 directly bound to three ABC transporter G family members (ABC-2, MRP10, ABCG37), mediating the efflux of the auxin precursor. The study showed that ABCG36 mediates the efflux of the auxin precursor indole 3-butyric acid (IBA) from roots, as evidenced by hypersensitive root growth phenotypes of *abcg36* mutants in the presence of IBA or precursors of synthetic auxin analogs in Arabidopsis (Strader *et al*., 2009; Ru□z□ic□ka *et al*., 2010). The function as a transporter of IBA and various auxinic compounds has also been assigned to ABCG37/PDR9, as evidenced by altered responsiveness of *abcg37* mutant plants to synthetic auxins and inhibitors of auxin transport, but not to IAA, the endogenous auxin (Ru□z□ic□ka *et al*., 2010; Ito and Gray, 2006; Strader *et al*., 2008). In this study, the qRT-PCR results showed that mRNA levels of ABC-2, MRP10, and ABCG37 were significantly higher in leaf pulvini of the ZmCLA4-RNAi plants than in WT plants. These results implied that ZmCLA4 could negatively regulate PAT by directly repressing ABC transporter G family members. Overall, these results suggest that ZmCLA4 represses ARF22 by

413 directly promoting IAA26 or directly repressing ABCGs or ARF22 and then mediated
414 auxin signal transduction, and finally led to a decrease in leaf angle.

415 The signaling pathways of various hormones in plants often cross each other,
416 forming a complex regulatory network. In terms of auxin, the interaction between BR,
417 ABA, JA, and other hormones has been extensively studied. In rice, OsLAZY1 plays
418 a negative role in PAT (Li *et al*., 2007). Except for ZmCLA4 directly binding to
419 ARF22 and IAA26 to participate in the pathway, ZmCLA4 not only mediates
420 brassinosteroid signal transduction through directly binding to BZR3 and 14-3-3 in
421 maize, but also binds to four genes (GTE8, SnRK2.6, WRKY4, WRKY72) in
422 response to ABA, two genes (CYP75B1 and CYP93D1) associated with JA, and two
423 genes (B3, ETO1) involved in the response to ethylene. In rice, the BR transcription
424 factor BZR1 increases leaf angle, whereas RNAi:BZR1 plants have leaves with small
425 inclinations (Bai *et al*., 2007; Zhang *et al*., 2012). BZR3, as a homologous gene of
426 BZR1, could increase the leaf angle in maize. BRs are a group of steroid hormones
427 with a paracrine mode of action that determines important traits, such as plant
428 architecture and have been extensively reported as key regulators of leaf angle in
429 cereals. This conclusion is derived from the numerous BR biosynthesis or signaling
430 mutants investigated in rice, maize, and sorghum with consistently reduced leaf
431 angles (Yamamuro *et al.*, 2000; Morinaka *et al.*, 2006; Sakamoto *et al.*, 2006; Wang
432 *et al.*, 2008; Divi and Krishna, 2009; Makarevitch *et al.*, 2012; Tong *et al.*, 2014; Sun
433 *et al.*, 2015; Best *et al.*, 2016; Feng *et al.*, 2016; Hirano *et al.*, 2017). The study of the
434 BR signaling pathway in Arabidopsis and rice is clear; that is, BR is sensed by BRI1

435 and its two homologous proteins BRL1 and BRL3. The unphosphorylated BKI1
436 interacts with BRI1, prevents the interaction between BRI1 and BAK1, and inhibits
437 the activation of BR signaling (Jiang *et al.*, 2015). BKI1 also competitively binds to
438 the 14-3-3 protein that assists in the degradation of BZR1, reducing the negative
439 regulatory effect of the 14-3-3 protein on BZR1, and then rapidly promotes the
440 transmission of the BR signal (Wang *et al*., 2011). Based on our data, mRNA levels
441 of BZR3 were significantly higher in ZmCLA4-RNAi plants than in the WT, and
442 mRNA levels of 14-3-3 were significantly lower in ZmCLA4-RNAi plants than in
443 WT plants, indicating that ZmCLA4 was involved in BRI1/BAK1 mediated BR
444 signaling by directly binding BZR3 and 14-3-3 to regulate leaf angle in maize.
445 Early evidence suggests that ABA reduces leaf angle and inhibits the action of
446 externally applied BRs (Wada *et al*., 1981). WRKYs include ABA-responsive
447 elements and might function as positive regulators in mediating plant responses to
448 ABA (Jiang and Deyholos, 2009; Gao *et al*., 2011). Accumulating evidence has
449 revealed that WRKY proteins play diverse roles in responses to biotic and abiotic
450 stresses and are involved in various processes of plant growth and development by
451 regulating the expression of target genes via binding to the W-box cis-element
452 (Rushton *et al*., 2010). For example, OsWRKY53 overexpression led to enlarged leaf
453 angles and increased grain size, in contrast to the erect leaves and smaller seeds in the
454 oswrky53 mutant (Tian *et al*., 2017). Based on our data, the mRNA levels of WRKY4
455 and WRKY72 were significantly higher in ZmCLA4-RNAi plants than in WT plants,
456 indicating that ZmCLA4 directly repressed the expression of ABA-responsive

457 WRKY4/72 (homologous gene of OsWRKY53) and mediated the ABA pathway to
458 reduce leaf angle in maize.

459 JAs also regulate leaf angles through their interaction with BR metabolism.
460 Methyl-JA represses the expression of BR biosynthesis and signaling genes, reducing
461 endogenous levels of BRs (Gan *et al.*, 2015), and thereby, leaf angle. CYP75B1 and
462 CYP93D1 were both annotated as "response to jasmonic acid (GO:0009753)." Heitz
463 *et al*. (2012) showed that cytochrome P450, CYP94C1, and CYP94B3 are involved in
464 JA-Ile oxidation. CYP93G1 converts naringenin to apigenin, and then CYP75B4
465 converts apigenin to luteolin, which is further metabolized to tricin through
466 *O*-methyltransferase activity and the chrysoeriol 5′-hydroxylase activity of CYP75B4
467 in rice (Lam *et al*., 2015; Sangkyu *et al*., 2016). Tricin derivatives have been reported
468 to be incorporated into lignin (Li *et al*., 2016). These results imply that ZmCLA4
469 directly regulates CYP75B1 and CYP93D1 (homologous genes of CYP75B and
470 CYP93G, respectively) to mediate the JA pathway and affect lignin biosynthesis,
471 thereby affecting the leaf angle in maize.

472 Ethylene is a gaseous plant hormone that plays a key role in leaf senescence
473 (Abeles *et al*., 1992). BR-induced rice lamina joint inclination was accompanied by
474 increased ethylene production because of greater expansion of the adaxial cells
475 relative to the dorsal cells in the lamina joint (Cao and Chen, 1995). We also found
476 that ZmCLA4 binds two genes (B3 and ETO1) involved in response to ethylene. In
477 particular, B3 encodes a B3 domain containing a protein homologous to ZmRAVL1
478 in maize (Tian *et al*., 2019). ZmRAVL1 RNAi and knockout lines exhibited smaller

leaf angles in the lower, middle, and upper leaves compared with that of the WT plants by increasing adaxial sclerenchyma cells in the ligular region (Tian *et al.*, 2019). From our data, B3 was significantly higher in ZmCLA4-RNAi plants than in WT plants. These results showed that ZmCLA4 decreased the leaf angle by directly repressing the expression of ethylene-responsive B3 in maize.

In summary, our results demonstrated that ZmCLA4, a cross node of five major phytohormone signaling pathways, negatively regulates leaf angle in maize. It directly affects the patterns of gene transcription. We built a hierarchical regulatory model describing ZmCLA4 and ZmCLA4-targeted genes to explain the effects on the formation of leaf angle during maize development. Our data suggest that ZmCLA4 directly represses genes associated with a range of biological responses, including auxin, BR, ABA, JA, and ethylene signaling pathways, resulting in an erect leaf angle. The manipulation of the regulation of leaf angle in maize reported herein, to adapt to high-density planting, has provided important insights that will help in directing future approaches for the production of high-yield maize varieties. A better understanding of ZmCLA4 regulatory pathways will provide new insights into the effects of ZmCLA4 through multiple signaling pathways in the future.

Acknowledgements

This research was supported by grants from the Central Plains Science and Technology Innovation Leading Talents (194200510021), National Key Research and

Development Program of China (2016YFD0101803) and National Natural Science Foundation of China (No. 31871639).

Author contributions

D.D., S. H. Z. R., D. Z., H. Z., Y. D., Z. L., F. Z., Q. Z., J. X. H. L. and H. C conducted molecular biology experiments; D. D. and H. S. analyze the data. Y. C, L.K., D. D. and S. H. designed the experiments and wrote the manuscript.

Conflict of interest

The authors declare they have no conflicts of interest.

Reference

Abeles F, Morgan P, Saltveit M. 1992. Ethylene in Plant Biology. Ethylene in plant biology. Academic Press, New York, USA.

Bai M, Zhang L, Gampala S, Zhu S, Song W, Chong K, Wang Z. 2007. Functions of OsBZR1 and 14-3-3 proteins in brassinosteroid signaling in rice. Proceedings of the National Academy of Sciences **104**, 13839-13844.

Best N, Hartwig T, Budka J, Fujioka S, Johal G, Schulz B, Dilkes B. 2016. nana plant2 encodes a maize ortholog of the Arabidopsis brassinosteroid biosynthesis gene DWARF1, identifying developmental interactions between brassinosteroids and gibberellins. Plant Physiology **171**, 2633–2647.

Cao Y, Zeng H, Ku L, Ren Z, Han Y, Su H, et al. 2020. ZmIBH1-1 regulates plant architecture in maize. Journal of Experimental Botany Doi: 10.1093/jxb/eraa052/5716501

Cao H, Chen S. 1995. Brassinosteroid-induced rice lamina joint inclination and its relation to indole-3-acetic acid and ethylene. Plant Growth Regulation **16**, 189-196.

524 **Chen X, Xu D, Liu Z, Yu T, Mei X, Cai Y.** 2015. Identification of QTL for leaf angle and leaf
525 space above ear position across different environments and generations in maize (Zea mays
526 L.). Euphytica **204**, 395–405.
527 **Chen Y, Fan X, Song W, et al.** 2011. Over-expression of OsPIN2 leads to increased tiller
528 numbers, angle and shorter plant height through suppression of OsLAZY1. Plant
529 Biotechnology Journal 10:139-149.
530 **Dharmasiri N, Dharmasiri S, Estelle M.** 2005a. The F-box protein TIR1 is an auxin receptor.
531 Nature **435**, 441-445.
532 **Dharmasiri N, Dharmasiri S, Weijers D, Lechner E, Yamada M, Hobbie L, Ehrismann J,**
533 **Jurgens G, Estelle M.** 2005b. plant development is regulated by a family of auxin receptor F
534 box proteins. Dev Cell **9**, 109-119
535 **Divi U, Krishna P.** 2009. Brassinosteroid: a biotechnological target for enhancing crop yield and
536 stress tolerance. New Biotechnology **26**, 131–136.
537 **Dong Z, Jiang C, Chen X, Zhang T, et al.** 2013. Maize LAZY1 Mediates Shoot Gravitropism
538 and Inflorescence Development through Regulating Auxin Transport, Auxin Signaling, and
539 Light Response. Plant Physiology **163**, 1306-22.
540 **Dubois P, Brutnell T.** 2011. Topology of a maize field: distinguishing the influence of
541 end-of-day far-red light and shade avoidance syndrome on plant height. Plant signaling &
542 behavior **6**, 467-470.
543 **Feng Z, Wu C, Wang C, et al.** 2016. SLG controls grain size and leaf angle by modulating
544 brassinosteroid homeostasis in rice. Journal of Experimental Botany **67**, 4241-4253.
545 **Gampala S, Hagenbeek D, Rock C.** 2001. Functional Interactions of Lanthanum and
546 Phospholipase D with the Abscisic Acid Signaling Effectors VP1 and ABI1-1 in Rice
547 Protoplasts. The Journal of biological chemistry **276**, 9855–9860.
548 **Garrett J, Meents M, Blackshaw M, Blackshaw L, Hou H, Styranko D, Schultz E.** 2012. A
549 novel, semi-dominant ′allele of MONOPTEROS provides insight into leaf initiation and vein
550 pattern formation. Planta **236**, 297–312.

Gao QM, Venugopal S, Navarre D, Kachroo A. 2011. Low oleic acid-derived repression of jasmonic acid-inducible defense responses requires the WRKY50 and WRKY51 proteins. Plant Physiol. **15**, 464–476.

Gan L, Wu, Wu D, et al. 2015. Methyl jasmonate inhibits lamina joint inclination by repressing brassinosteroid biosynthesis and signaling in rice. Plant Science **241**, 238-245.

Heitz T, Widemann E, Lugan R, et al. 2012. Cytochromes P450 CYP94C1 and CYP94B3 Catalyze Two Successive Oxidation Steps of Plant Hormone Jasmonoyl-isoleucine for Catabolic Turnover. Journal of Biological Chemistry 287, 6296-6306.

Hirano K, Kawamura M, Araki-Nakamura S, Fujimoto H, Ohmae- Shinohara K, et al. 2017. Sorghum DW1 positively regulates brassinosteroid signaling by inhibiting the nuclear localization of BRASSINOSTEROID INSENSITIVE 2. Scientific Reports **7**, 126.

Ito H, Gray, W. 2006. A gain-of-function mutation in the Arabidopsis pleiotropic drug resistance transporter PDR9 confers resistance to auxinic herbicides. Plant Physiol. **142**, 63-74

Jiang J, Wang T, Wu Z, et al. 2015. The intrinsically disordered protein BKI1 is essential for inhibiting BRI1 signaling in plants. Mol Plant **8**, 1675-1678

Jiang Y, Deyholos M. 2009. Functional characterization of Arabidopsis NaCl-inducible WRKY25 and WRKY33 transcription factors in abiotic stresses; Plant Mol. Biol. **69**, 91-105

Kazan K. 2006. Negative regulation of defense and stress genes by EAR-motif-containing repressors. Trends Plant Sci. **11**, 109-112.

Kagale S, Links M, Rozwadowski K. 2010. Genome-wide analysis of ethylene-responsive element binding factor-associated amphiphilic repression motif-containing transcriptional regulators in Arabidopsis. Plant Physiol. **152**, 1109-1134.

Kepinski S, Leyser O. 2005. The Arabidopsis F-box prorein TIR1 is an auxin receptor. Nature **435**, 446-451

Kepinski S, Leyser O. 2005. Plant Development: Auxin in Loops. Current Biology **15**, 208-210.

Ku L, Zhao W, Zhang J, Wu L, Wang C, Wang P, Zhang W, Chen. 2010. Quantitative trait loci mapping of leaf angle and leaf orientation value in maize (Zea mays L.). Theoretical and Applied Genetics **121**, 951-959.

Ku L, Zhang J, Guo S, et al. 2012. Integrated multiple population analysis of leaf architecture traits in maize (Zea mays L.). Journal of Experimental Botany, 63, 261-274.

Ku L, Wei X, Zhang S, Zhang J, Guo S, Chen Y. 2011. Cloning and characterization of a putative TAC1 ortholog associated with leaf angle in maize (Zea mays L.). PLoS One 6, e20621.

Lambert R, Johnson R. 1978. Leaf angle, tassel morphology, and the performance of maize hybrids. Crop Sci, 818, 499-502

Lam P, Liu H, Lo C. 2015. Completion of tricin biosynthesis pathway in rice: Cytochrome P450 75B4 is a unique chrysoeriol 5′-hydroxylase. Plant Physiol. **168**, 1527-1536.

Langmead B, Salzberg SL. 2012. Fast gapped-read alignment with Bowtie 2. Nature methods 9, 357-359.

Li C, Li Y, Shi Y, Song Y, Zhang D, Buckler E, Zhang Z, Wang T, Li Y. 2015. Genetic control of the leaf angle and leaf orientation value as revealed by ultra-high density maps in three connected maize populations. PLoS One **10**, 1-13.

Li M, Pu Y, Yoo C, Ragauskas A. 2016. The occurrence of tricin and its derivatives in plants. Green Chem. 18, 1439-1454.

Li PJ, Wang YH, Qian Q, Fu Z, Wang M, Zeng D, Li B, Wang X, Li J. 2007. LAZY1 controls rice shoot gravitropism through regulating polar anxin transport. Cell Research **17**, 402-410.

Li Z, Liang Y, Yuan Y, Wang L, Meng X, Xiong G, Zhou J, Cai Y, Han N, Hua L, Liu G, Li J., and Wang Y. 2019. OsBRXL4 Regulates Shoot Gravitropism and Rice Tiller Angle through Affecting LAZY1 Nuclear Localization. Mol. Plant. **12**, 1143-1156.

Lu M, Zhou F, Xie CX, Li MS, Xu YB, Marilyn W, Zhang SH. 2007 Construction of a SSR linkage map and mapping of quantitative trait loci (QTL) for leaf angle and leaf orientation with an elite maize hybrid. Hereditas **29**, 1131-1138.

Makarevitch I, Thompson A, Muehlbauer GJ, Springer NM. 2012. Brd1 gene in maize encodes a brassinosteroid C-6 oxidase. PLoS One **7**, e30798.

McCormick RF, Truong SK, Mullet JE. 2016. 3D Sorghum reconstructions from depth images identify QTL regulating shoot architecture. Plant Physiology **172**, 823-834.

607 **Mickelson SM, Stuber CS, Senior L, Kaeppler SM.** 2002. Quantitative trait loci controlling leaf
608 and tassel traits in a B73×MO17 population of maize. Crop Science **42**, 1902-1909.
609 **Morinaka Y, Sakamoto T, Inukai Y, getsuma M, Kitano H, Ashikari M, Matsuoka M.** 2006.
610 Morphological alteration caused by brassinosteroid insensitivity increases the biomass and
611 grain production of rice. Plant Physiology **141**, 924-931.
612 **O' Malley RC, Huang SS Song L, et al.** 2016. Cistrome and Epicistrome Features Shape the
613 Regulatory DNA Landscape. Cell **165**, 1280-1292.
614 **Ohta M.** 2001. Repression Domains of Class II ERF Transcriptional Repressors Share an
615 Essential Motif for Active Repression. The Plant Cell, 13, 1959-1968.
616 **Ren Z, Wu L, Ku L, Wang H, Zeng H, e al,** 2020, ZmILI1 regulates leaf angle by directly
617 affecting liguleless1 expression in maize. Plant Biotechnology Journal. **18**, 881-883
618 **Ru□z□ic□ka K. et al.** 2010. Arabidopsis PIS1 encodes the ABCG37 transporter of auxinic
619 compounds including the auxin precursor indole-3- butyric acid. Proc. Natl. Acad. Sci. **107**,
620 10749–10753 (2010).
621 Rushton PJ, Somssich IE, Ringler P, Shen QJ. 2010. WRKY transcription factors. Trends Plant
622 Sci **15**, 247–258
623 **Sakamoto T, Morinaka Y, Ohnishi T, et al.** 2006. Erect leaves caused by brassinosteroid
624 deficiency increase biomass production and grain yield in rice. Nature Biotechnology **24**,
625 105–109.
626 **Sangkyu P, Min C, Jong L, et al.** 2016. Molecular and Biochemical Analysis of Two Rice
627 Flavonoid 3'-Hydroxylase to Evaluate Their Roles in Flavonoid Biosynthesis in Rice Grain.
628 International Journal of Molecular Sciences **17**, 1549-1553.
629 **Strader L, Bartel B.** 2009. The Arabidopsis PLEIOTROPIC DRUG RESISTANCE8/ABCG36
630 ATP binding cassette transporter modulates sensitivity to the auxin precursor
631 indole-3-butyric acid. Plant Cell **21**, 1992–2007.
632 **Strader L, Monroe-Augustus M, Rogers K, Lin G, Bartel B.** 2008. Arabidopsis iba response5
633 suppressors separate responses to various hormones. Genetics **180**, 2019-2031.

Sun S, Chen D, Li X, Qiao S, Shi C, Li C, Shen H, Wang X. 2015. Brassinosteroid signaling regulates leaf erectness in Oryza sativa via the control of a specific U-type cyclin and cell proliferation. Developmental Cell **34**, 220–228.

Tian F, Bradbury P, Brown P, Hung H, Sun Q. Flint-Garcia S, Rocheford T, McMullen MD. Holland J, Buckler E. 2011 Genome-wide association study of leaf architecture in the maize nested association mapping population. Nature Genetics **43**, 159-162.

Tian J, Wang C, Xia J, Wu L, Xu G, Wu W et al. 2019. Teosinte ligule allele narrows plant architecture and enhances high-density maize yields. Science **365**, 658-664.

Tian X, Li X, Zhou W, et al. 2017. Transcription factor OsWRKY53 positively regulates brassinosteroid signaling and plant architecture. Plant Physiology 00946.

Tiwari SB, Wang X-J, Hagen G, Guilfoyle TJ. 2001. AUX/IAA Proteins Are Active Repressors, and Their Stability and Activity Are Modulated by Auxin. The Plant cell **13**, 2809–2822.

Tong H, Xiao Y, Liu D, Gao S, Liu L, Yin Y, Jin Y, Qian Q, Chu C. 2014. Brassinosteroid regulates cell elongation by modulating gibberellin metabolism in rice. The Plant Cell **26**, 4376-4393.

Wang L, Xu Y, Zhang C, Ma Q, Joo SH, Kim SK, Xu Z, Chong K. 2008. OsLIC, a novel CCCH-type zinc finger protein with transcription activation, mediates rice architecture via brassinosteroids signaling. PLoS One **3**, e3521.

Wang H, Yang C, Zhang C, et al. 2011. Dual role of BKI1 and 14-3-3 s in brassinosteroid signaling to link receptor with transcription factors. Dev Cell **21**, 825–834

Wada K, Marumo S, Ikekawa N, Morisaki M, Mori K. 1981. Brassinolide and homobrassinolide promotion of lamina inclination of rice seedlings. Plant and Cell Physiology **22**, 323-325.

Yang C, Xie F, Jiang Y, et al. 2018. Phytochrome A negatively regulates the shade avoidance response by increasing auxin/indole acidic acid protein stability. Dev Cell, **44**, 29-41.e4

Yamamuro C, Ihara Y, Wu X, Noguchi T, Fujioka S, Takatsuto S, Ashikari M, Kitano H, Matsuoka M. 2000. Loss of function of a rice brassinosteroid insensitive1 homolog prevents internode elongation and bending of the lamina joint. The Plant Cell **12**, 1591–1606.

662 **Yoshihara T, Iino M.** 2007. Identification of the gravitropism-related rice gene LAZY1 and
663 elucidation of LAZY1-dependent and -independent gravity signaling pathways. Plant and
664 Cell Physiology **48**, 678-688.
665 **Yoshihara T, Spalding EP, Iino M.** 2013. AtLAZY1 is a signaling component required for
666 gravitropism of the Arabidopsis thaliana inflorescence. The Plant Journal **74**, 267-279.
667 **Zhang C, Xu Y, Guo S, Zhu J, Huan Q, Liu H, Wang L, Luo G, Wang X, Chong K.** 2012.
668 Dynamics of brassinosteroid response modulated by negative regulator LIC in rice. PLoS
669 Genetics **8**, e1002686.
670 **Zhang J, Ku L X, Han Z P, et al.** 2014. The ZmCLA4 gene in the qLA4-1 QTL controls leaf
671 angle in maize (Zea mays L.). Journal of Experimental Botany 65, 5063-5076.
672 **Zhang N, Yu H, Yu H, et al.** 2018. A Core Regulatory Pathway Controlling Rice Tiller Angle
673 Mediated by the LAZY1-dependent Asymmetric Distribution of Auxin. The Plant Cell **30**,
674 1461-1475.
675 **Zhang S, Wang S, Xu Y, et al.** 2015. The auxin response factor, OsARF19, controls rice leaf
676 angles through positively regulating OsGH3-5 and OsBRI1. Plant, Cell & Environment 38,
677 638-654.
678 **Zhang X, Huang C. Wu D, et al.** 2017. High-throughput phenotyping and QTL mapping reveals
679 the genetic architecture of maize plant growth. Plant Physiology **173**, 1554-1564.
680 **Zhang Y, Liu T, Meyer CA, et al.** 2008. Model-based analysis of ChIP-Seq (MACS). Genome
681 biology 9, R137.
682
683
684
685
686
687

688

689

690

691

692

693

694

695 **Figure legends**

696 **Fig. 1. Characteristic analysis of ZmCLA4 protein.**

697 **(A)** Sequence alignment of maize CLA4, rice LAZY1, and Arabidopsis AtLAZY1

698 amino acid sequences. The alignment was performed using DNAMAN. Identical

699 amino acids are in black and the conserved EAR motif is underlined in red. **(B)**

700 Transactivation analysis of ZmCLA4 fused to the GAL4 DNA-binding domain in

701 yeast. **(C)** Transient assays of the transcriptional activity of ZmIBH1-1. *Nicotiana*

702 *benthamiana* leaves were transformed with the reporter (UAS-LUC) and effector

703 constructs (left), and the reporter gene expression was determined (right). Data are

704 means (± SD), n = 3. UAS-LUC, reporter construct containing Gal4 and LexA

705 binding sites, and a 35S minimal promoter upstream of the coding sequence of LUC;

706 VP16, VP16 fused to the LexA DNA-binding domain (DBD); Gal4, Gal4 DBD;

707 IAA17a1, the transcription repression domain of IAA17 fused to the Gal4 DBD;

708 ZmCLA4, full-length ZmCLA4 fused to Gal4 DBD. The LUC reporter gene

expression was normalized to the luciferase activity and presented as values relative to the VP16 control, the value of which was set as 1.

Fig. 2. DAP-seq analysis of maize *ZmCLA4*.

(A) ZmCLA4 binding to CACCGGAC, CCGARGS, and CDTCNTC motifs as identified by the MEME-ChIP. **(B)** Distribution of the ZmCLA4 binding sites. **(C)** Comparison of ZmCLA4-occupied peaks using two biological replicates. **(D)** GO annotation of targeted genes bound by ZmCLA4. The y-axis represents the percentage of genes related to each functional category. **(E)** Results of EMSAs confirming ZmCLA4 binding to CACCGGAC, CCGARGS, and CDTCNTC.

Fig. 3. ZmCLA4 functions as a transcriptional repressor of the genes involved in response to auxins.

(A) The 35S:REN-Pro PR:LUC reporter constructs were transiently expressed in *Nicotiana benthamiana* leaves together with the control vector or 35S: ZmCLA4 effector. **(B)** The LUC/REN ratio represents the relative activity of the gene promoters (*P < 0.05, **P < 0.01). **(C)** Expression analysis of the targeted genes in wild-type and ZmCLA4-RNAi plants using leaf pulvini from the 9-leaf, 10-leaf, and 11-leaf stages.

Fig. 4. ZmCLA4 functions as a transcriptional repressor of the genes involved in response to brassinolide.

(A) The LUC/REN ratio represents the relative activity of the gene promoters (*P < 0.05, **P < 0.01). **(B)** Expression analysis of the targeted genes involved in responses

730 to brassinolide in wild-type and ZmCLA4-RNAi plants using leaf pulvini from the
731 9-leaf, 10-leaf, and 11-leaf stages.

732 **Fig. 5. ZmCLA4 functions as a transcriptional repressor of other**
733 **phytohormone-related genes.**

734 **(A)** The LUC/REN ratio represents the relative activity of the gene promoters (*P <
735 0.05, **P < 0.01). **(B)** Expression analysis of the other phytohormone-respective
736 targeted genes in wild-type and ZmCLA4-RNAi plants using leaf pulvini from the
737 9-leaf, 10-leaf, and 11-leaf stages.

738 **Fig. 6. A schematic model for leaf angle formation in maize.**

739 The arrows between the genes represent promotion or activation, and the ⊥ bars
740 between the genes indicate suppression. The green circles represent auxin-responsive
741 genes, the yellow circle represents the jasmonic acid-responsive gene, the bright green
742 circles represent the brassinosteroid-responsive genes, the orange circles represent
743 ethylene-responsive genes, and the lavender circle represents the abscisic
744 acid-responsive genes.

745

746 **Supporting information**

747 The following materials are available in the online version of this article.

748 **Table S1. Primer sequences used for the experiments.**

749 **Table S2. The summary of reads analysis.**

750 **Table S3. CLA4 regulating leaf angle-related genes in maize.**

751

752

753

754

755

756

757

758

759

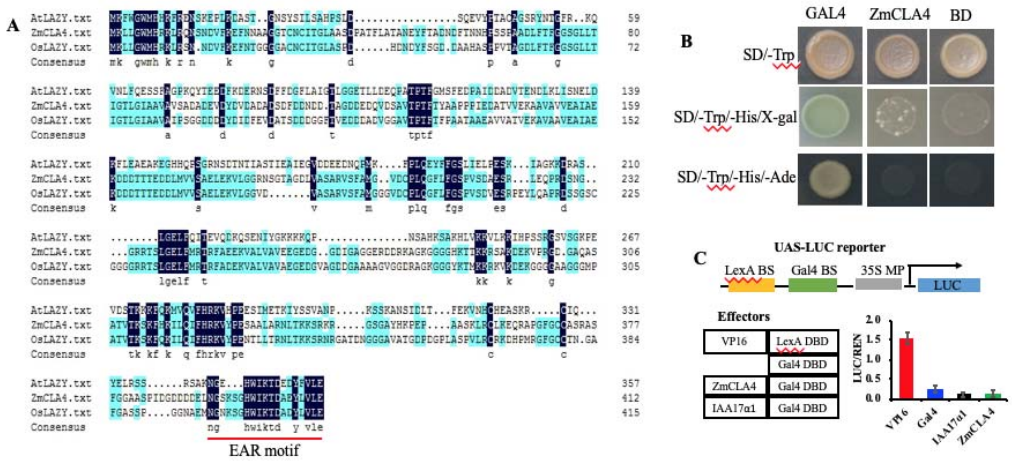

760

761 **Fig. 1. Characteristic analysis of ZmCLA4 protein.**

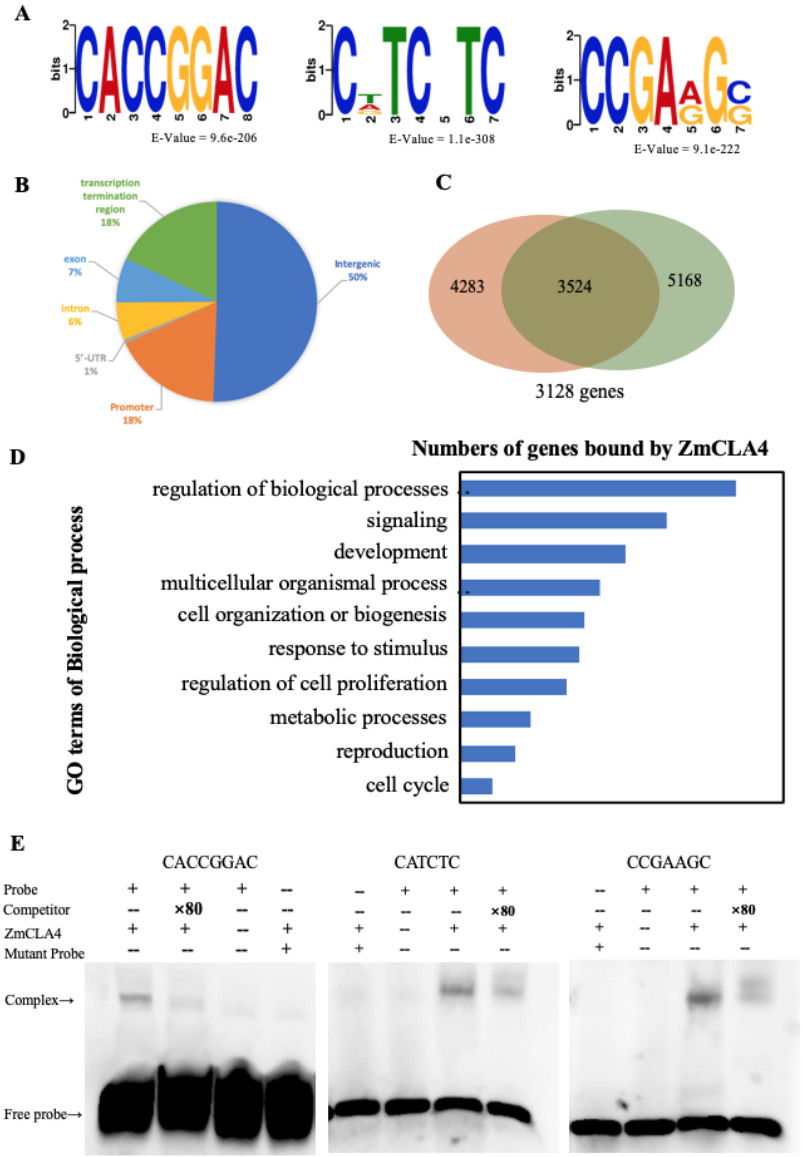

762

763 **Fig. 2. DAP-seq analysis of maize *ZmCLA4*.**

764

765

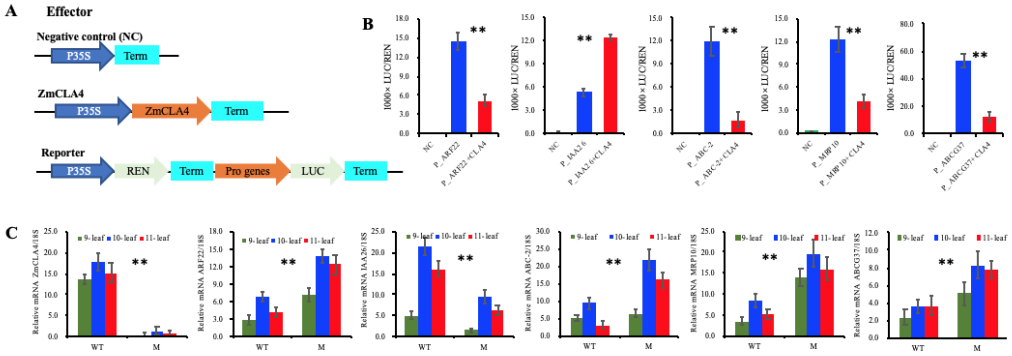

766

767 **Fig. 3. ZmCLA4 functions as a transcriptional repressor of the genes involved in**

768 **response to auxins.**

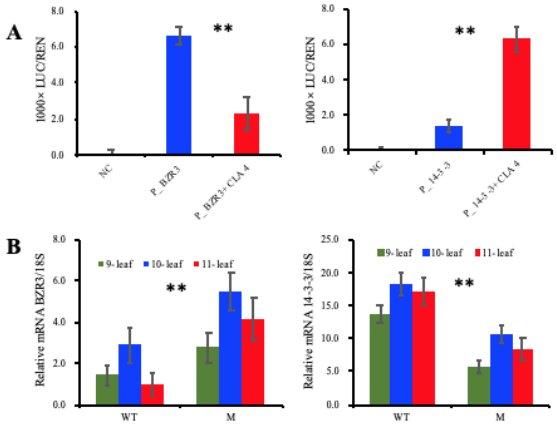

769

770 **Fig. 4. ZmCLA4 functions as a transcriptional repressor of the genes involved in**

771 **response to brassinolide.**

772

773

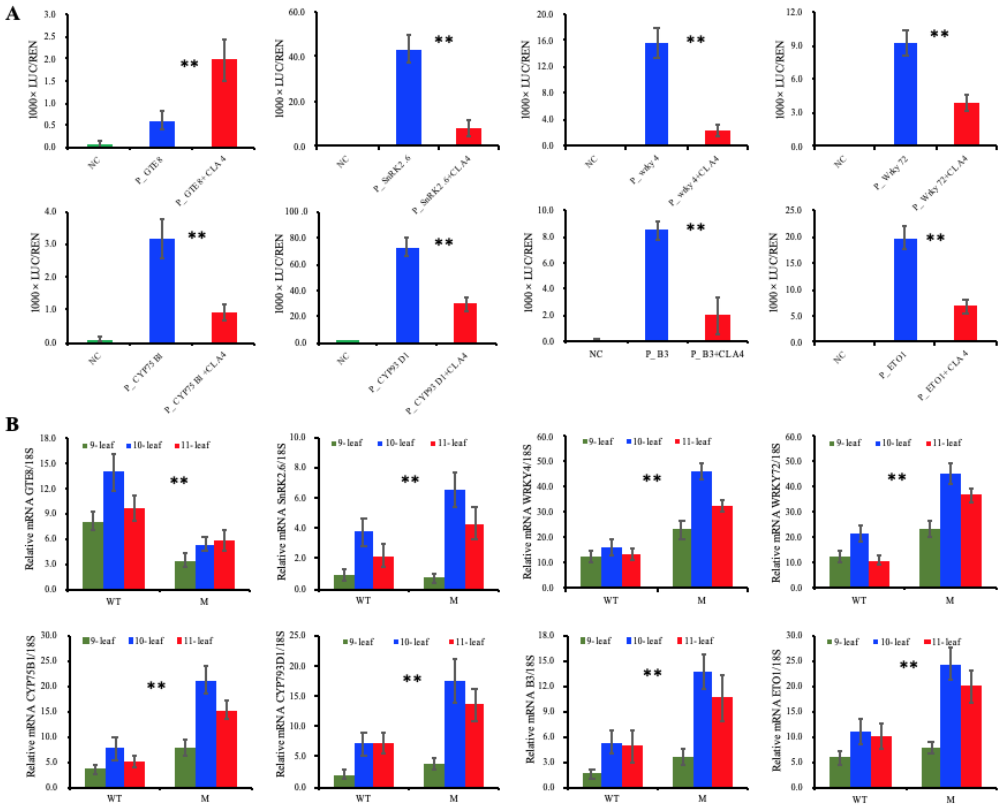

774

775 **Fig. 5. ZmCLA4 functions as a transcriptional repressor of other**

776 **phytohormone-related genes.**

777

778

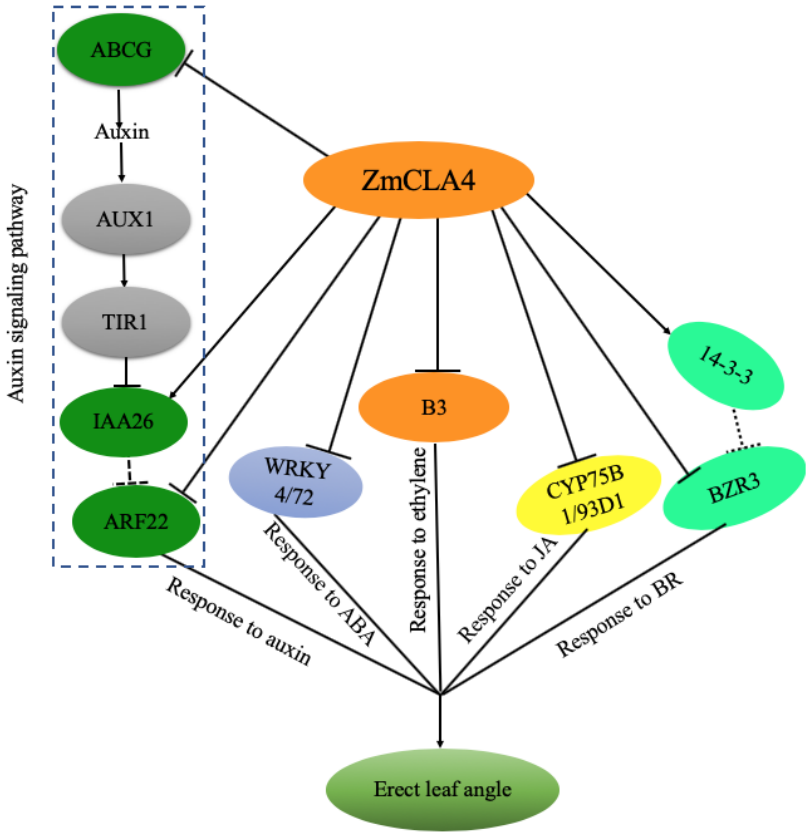

779

780 **Fig. 6. A schematic model for leaf angle formation in maize.**